A Self-Packaged SISL Low-Power Rectifier Based on a High-Impedance Line for *C*-Band Applications

Dingnan Liu, Ling Wang, Zhongqi He, and Changjun Liu, *Senior Member, IEEE*

***Abstract*—In this letter, a self-packaged substrate-integrated suspended line (SISL) rectifier is proposed. The rectifier consists of a quarter-wavelength high-impedance transmission line, a diode, a tuning inductor, and a dc pass filter. The lower the power is, the lower the rectifying efficiency is. At a low input power level, the diode impedance real part is almost zero. A tuning inductor is introduced to form a parallel resonator to enhance the diode voltage. A quarter-wavelength high-impedance line is presented to match the rectifying diode to the source. In addition, due to the self-packaging characteristics and air cavity of SISLs, the radiation loss and dielectric loss of the proposed rectifier are reduced. A rectifier was designed, fabricated, and measured at 5.8 GHz. The radio frequency (RF)-dc conversion efficiency reaches 3.5% at −30 dBm, which is close to its theoretical estimated efficiency at 5.8 GHz. This ultralow power rectifier may be used in energy harvesting at *C*-band.**

***Index Terms*—High impedance line, rectifier, radio frequency (RF)-dc conversion efficiency, substrate integrated suspended line (SISL), ultralow power.**

I. Introduction

With the rapid development of the Internet of Things (IoT), wireless sensor networks, biomedical implant systems, and intelligent transportation systems in recent years, a large number of low-power and miniaturized wireless sensors are distributed in all corners of the world [1], [2]. Using batteries to power sensors increases the size of devices and is not sustainable and practically impossible. Due to the wide application of power sources such as cellular mobile base stations and radio frequency (RF) signal tower, the space is flooded with a large amount of RF energy [3]. Ambient RF energy harvesting is expected to solve the power supply problem of electronic systems in some emerging application fields [4], [5], [6], [7], [8], [9], [10], [11], [12], [13], [14], [15], [16], [17], [18], [19]. Because the power spectrum of signals in the environment is relatively low with a typical power density of 2 μW/m^2–10 mW/m^2 [20], the rectifiers are required to have excellent RF-dc conversion performance at a much low input power range.

In addition, in the 1950s, Glaser [21] put forward the solar satellite plan. The solar satellite project hopes to use solar energy to power electronic components on the Earth through microwave power transmission, in an effort to solve the resource shortage facing humanity [22]. Low-orbit near-Earth satellites for the space solar power satellite (SSPS) verification are planned to launch in the future. The microwave power transmission may be at 5.8 GHz. The power density on the ground is very low due to the limitation of the transmitting antenna aperture and the transmitted power level. It requires microwave rectifiers working at ultralow power level, e.g., about −30 dBm.

Manuscript received 10 June 2022; revised 15 August 2022; accepted 10 September 2022. Date of publication 18 October 2022; date of current version 13 February 2023. This work was supported by the National Natural Science Foundation of China (NSFC) under Grant 62071316 and Grant 61931009. *(Corresponding author: Changjun Liu.)*

The authors are with the School of Electronics and Information Engineering, Sichuan University, Chengdu 610064, China, and also with the Yibin Industrial Technology Research Institute, Sichuan University, Yibin 644001, China (e-mail: cjliu@ieee.org.).

Color versions of one or more figures in this letter are available at https://doi.org/10.1109/LMWC.2022.3211180.

Digital Object Identifier 10.1109/LMWC.2022.3211180

TABLE I
Performance With the Prior Rectifiers

Ref.	f (GHz)	Diode	Efficiency @ -40 dBm and -30 dBm			
			-40 dBm		-30 dBm	
			Measure	Estimate	Measure	Estimate
[26]	2.35	Tunnel diode	3.8%	2.1%	18.2%	21.5%
[29]	0.9	SMS7630	3%	4%	17.5%	40.4%
[34]	1.9	VDI ZBD	1.8%	2.7%	11.2%	27.1%
This work	**5.8**	**SMS7630**	**1.2%**	**0.3%**	**3.5%**	**3.14%**

Multifarious effective methods have been adopted to enhance the efficiency of ultralow power rectifiers. For example, hybrid energy collection exacerbating a nonlinear process in the diode was a significant method to increase the RF-dc conversion efficiency of energy harvesters [23], [24]. Also, some diodes with a strong nonlinearity such as tunnel diodes [25], nanodiodes [26], and spin diodes [27] were used to elevate efficiency. However, it is very challenging to break the rectifying efficiency limitation by ameliorating the diode manufacturing process. Moreover, the RF-dc conversion efficiency of rectifiers was raised by making the diodes operate at the optimum temperature [28], [29]. The above rectifiers are all operating in the *S*-band and below. There are few research studies on *C*-band with a typical power of −30 dBm and below, where conversion efficiency is so limited.

The substrate-integrated suspended line (SISL) technology can reduce radiation loss and dielectric loss significantly [30], and has been used for voltage-controlled oscillators (VCOs) [31], LNAs [32], and other circuits. In this letter, an SISL rectifier based on a high impedance line is proposed at 5.8 GHz. The impedance matching network of the rectifier is uncomplicated and easy to implement. The measured results show that the proposed SISL rectifier achieves an RF-dc conversion efficiency of 3.5% at −30 dBm. Table I shows the estimated theoretical efficiency of an SMS7630 diode at different frequencies calculated by (1) and the comparison between the proposed rectifier and previous work.

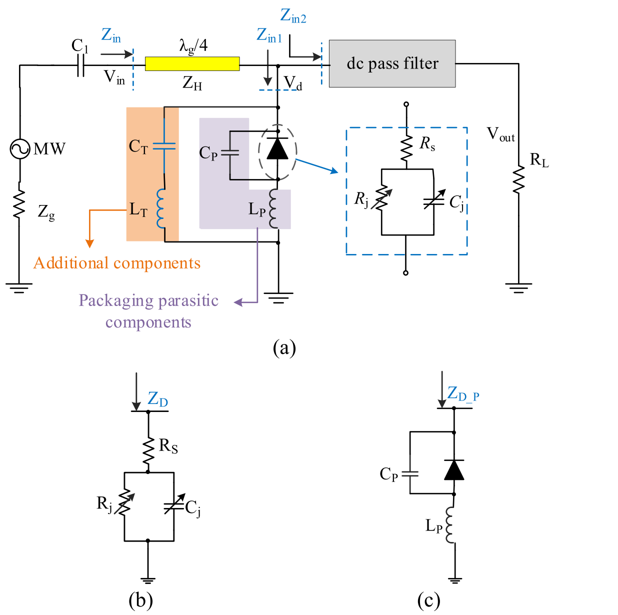

Fig. 1. (a) Schematic of the proposed rectifier. (b) Diode impedance without packaging parameters. (c) Diode impedance with packaging parameters.

TABLE II
SPICE AND PACKAGING PARAMETER OF DIODE SMS7630-079LF

Parameter	I_S	R_S	C_{j0}	V_{bi}	L_P	C_P
Unit	A	Ω	pF	V	nH	pF
Value	5×10^{-6}	20	0.14	0.34	0.70	0.16

II. Principle and Design Method

A. Principle

The square-law rectification model presented in [27] can be applied to the efficiency analysis of rectifiers at such a low-power level. Selecting an optimum load and neglecting the matching losses, the estimated theoretical efficiency η can be calculated by [27]

$$\eta = \frac{P_j \cdot \Re_{I0}^2 \cdot R_{j0}}{4} . \frac{1}{\left(1+\left(\omega . C_{j0}\right)^2 . R_s . R_{j0}\right)^2} \tag{1}$$

where P_j is the RF power transferred to the junction resistance; for SMS7630 diodes, $\Re_{I0}$ is 18.42 A/W, the diode zero-bias current responsivity; R_{j0} is 5430 Ω, the junction resistance at zero-bias. R_S, C_{j0}, and ω represent the series resistance, junction capacitance at zero bias, and angular frequency, respectively.

The diagram of the proposed rectifier is shown in Fig. 1(a). It consists of a quarter-wavelength high-impedance transmission line, a rectifying diode, a tuning inductor, and a dc pass filter. Table II shows the SPICE and packaging parameters of the rectifying diode SMS7630-079LF.

The proposed SISL rectifier based on a high-impedance line owns advantages.

1) Low Loss SISL: Fig. 2 displays the 3-D view of the SISL rectifier. It is made up of five printed circuit boards (PCBs). Copper foil layers are connected through via holes. Sub2 and Sub4 are FR4 with a thickness of 1.6 mm to reserve enough space to weld capacitors and diodes, and are hollowed out to form two air cavities. The core circuit is located at G5. The electric field of the SISL rectifier is mainly distributed in the air cavity instead of the substrate, which reduces the dielectric loss greatly. The radiation loss is obviously depressed due to the air cavity enclosed by the embedded metallic via-holes and top-and-bottom ground. In addition, the multilayer structure of the SISL makes it easy to integrate with other circuits.

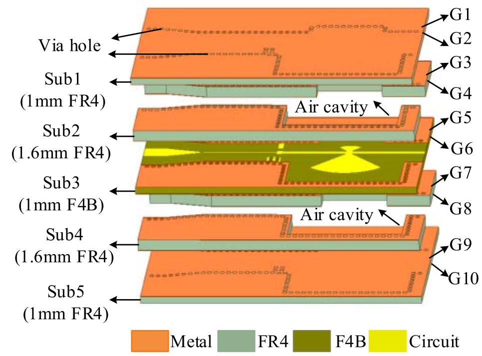

Fig. 2. 3-D view of the proposed rectifier.

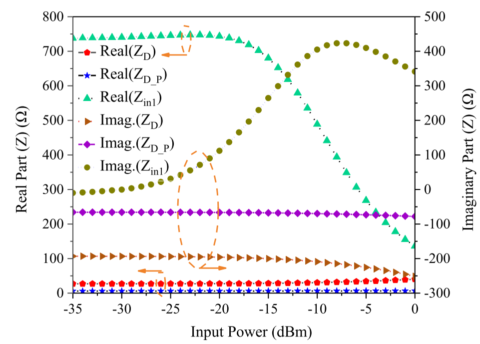

Fig. 3. Simulated impedance variation with input power in ADS.

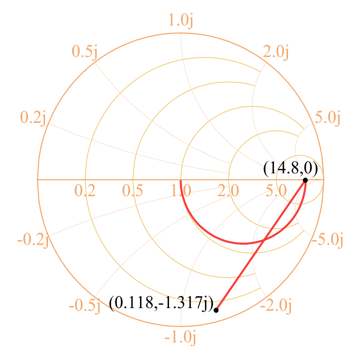

Fig. 4. Impedance matching process from the diode to source in normalized Smith chart.

2) High Impedance Transmission Line: The simulated impedance variation, e.g., the diode impedance with/without packaging and tuning inductor as shown in Fig. 1, with respect to input power in advanced design system (ADS) is shown in Fig. 3. The real part of Z_{in1} reaches several hundred ohms with the introduction of the tuning inductor. A quarter-wavelength high-impedance transmission line matches the diode to the source, which makes the matching network uncomplicated and facilitated. Fig. 4 illustrates the impedance matching process

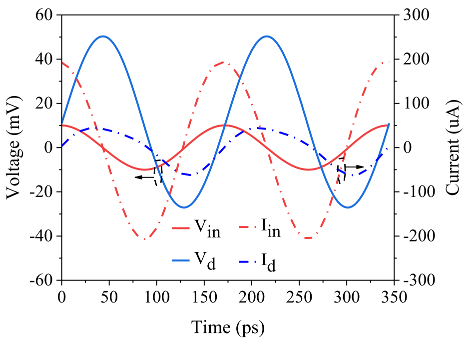

Fig. 5. Simulated voltage and current waveforms of the proposed rectifier at −30 dBm.

from the rectifying diode to the source in a normalized Smith chart. As can be observed in Fig. 5, the peak value of the diode voltage V_d is about four times the input voltage V_{in} at −30 dBm, which contributes to rectifying [34].

B. Rectifier Design

The impedance matching network of the proposed rectifier is specifically designed for the input power level of −30 dBm. At such a low power level, the diode cannot be considered an ideal switch anymore [28]. The Schottky diode impedance Z_D is given by

$$Z_D = R_S + \frac{R_j}{1 + j\omega C_j . R_j} \tag{2}$$

where R_j and C_j are the diode resistance and capacitance, respectively. They are approached by their zero-bias values. Considering the parasitic elements L_P and C_P, the whole impedance Z_{D_P} is

$$Z_{D\_P} = \frac{Z_D}{1 + j\omega C_p . Z_D} + j\omega L_P. \tag{3}$$

After employing the tuning inductor L_T and the dc blocking capacitor C_T, the input impedance $Z_{\text{in}1}$ of the rectifying branch is

$$Z_{\text{in}1} = \frac{Z_{D\_P}\left(1 - \omega^2 L_T C_T\right)}{1 - \omega^2 L_T C_T + j\omega C_T . Z_{D\_P}}. \tag{4}$$

C_T is 3 pF. L_T is 2.09 nH, which is obtained by solving $\text{Im}[Z_{\text{in}1}] = 0$. Therefore, $Z_{\text{in}1}$ is 755 Ω. The dc-pass filter shows a high impedance at the fundamental frequency. Thus, $Z_{\text{in}2}$ is infinity and is neglected.

Then, a quarter-wavelength transmission line is applied to impedance matching. Z_H is the characteristic impedance of the quarter-wavelength transmission line, calculated by

$$Z_H = \sqrt{Z_g Z_{\text{in}1}} \tag{5}$$

where Z_g is 50 Ω. Z_H is 194 Ω, which is difficult to implement by a microstrip line.

III. Implementation

The fabricated rectifier consists of five PCBs in Fig. 6. Five PCBs are secured and compacted with screws. The core circuit is located in G5. Substrate F4B is with a loss tangent of 0.002, with a thickness of 1 mm, and a relative dielectric constant of 2.65. It was used as Sub3. Substrate FR4 was used for Sub1, Sub2, Sub4, and Sub5. The thickness is 1 mm for Sub1 and Sub5, and 1.6 mm for Sub2 and Sub4. The fabricated rectifier is 40 × 25 × 6.2 mm. It is a little bulky and complex using the SISL structure compared with microstrip line rectifiers without metal cavity.

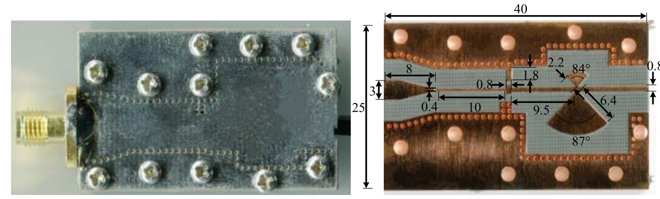

Fig. 6. Photograph of the fabricated rectifier (unit: mm).

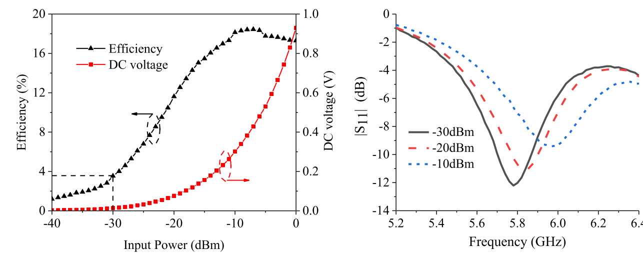

(a) (b)

Fig. 7. (a) Measured RF-dc conversion efficiency and output dc voltage versus input power at 5000 Ω load. (b) Measured $|S_{11}|$ versus frequency at different input power level.

A 3 pF capacitor C_1 is used as dc blocking. A short-ended transmission line is applied to realizing inductor L_T. Its width and length are 0.8 and 1.7 mm, respectively. The quarter-wavelength high-impedance transmission line with an optimized width of 0.4 mm serves as the matching network. The dc pass filter is implemented by a quarter-wavelength transmission line and two fan branches. All lengths and widths of microstrip lines were optimized for RF-dc conversion efficiency.

IV. Experimental Results

The proposed rectifier was designed, fabricated, and measured at 5.8 GHz with a 5000 Ω load. A microwave source (Agilent E8267C) was used to generate the RF power. The output dc voltage was measured by a voltage meter. Fig. 7(a) shows the RF-dc conversion efficiency is 3.5%, 11.6%, and 18.1% at the input power at −30, −20, and −10 dBm, respectively.

A vector network analyzer (VNA, Agilent N5230A) was applied to measure S-parameter. Fig. 7(b) depicts the measured $|S_{11}|$ from 5.2 to 6.4 GHz at the input power level at −30, −20, and −10 dBm, respectively. The optimal frequency is dependent on the input RF power. When the input RF power is −30 dBm, the measured $|S_{11}|$ reaches −12 dB at 5.8 GHz.

V. Conclusion

In this letter, a low loss and self-packaged SISL rectifier is proposed. A quarter-wavelength high-impedance transmission line acting as an impedance matching network makes the rectifier facilitated. The proposed topology has a good performance at an input low-power level. The measured efficiency reaches 3.5% at −30 dBm input power. The fabricated rectifier is 40 × 25 mm. It may be applied to the ultralow power conversion in future low-earth orbit solar power satellite (LEO SPS) demo system.

References

[1] M. R. Elhebeary, M. A. A. Ibrahim, M. M. Aboudina, and A. N. Mohieldin, "Dual-source self-start high-efficiency microscale smart energy harvesting system for IoT," *IEEE Trans. Ind. Electron.*, vol. 65, no. 1, pp. 342–351, Jun. 2018.

[2] M. Kumar, S. Kumar, and A. Sharma, "Dual-purpose planar radial-array of rectenna sensors for orientation estimation and RF-energy harvesting at IoT nodes," *IEEE Microw. Wireless Compon. Lett.*, vol. 32, no. 3, pp. 245–248, Mar. 2022.

[3] P. Lu, C. Song, and K. M. Huang, "A compact rectenna design with wide input power range for wireless power transfer," *IEEE Trans. Power Electron.*, vol. 35, no. 7, pp. 6705–6710, Jul. 2020.

[4] Y. Huang, N. Shinohara, and H. Toromura, "A wideband rectenna for 2.4 GHz-band RF energy harvesting," in *Proc. IEEE Wireless Power Transf. Conf. (WPTC)*, May 2016, pp. 1–3.

[5] A. Adeyeye, C. Lynch, A. Eid, J. Hester, and M. Tentzeris, "5.8-GHz low-power tunnel-diode-based two-way repeater for non-line-of-sight interrogation of rfids and wireless sensor networks," *IEEE Microw. Wireless Compon. Lett.*, vol. 31, no. 6, pp. 794–797, Jun. 2021.

[6] Z. He and C. Liu, "A compact high-efficiency broadband rectifier with a wide dynamic range of input power for energy harvesting," *IEEE Microw. Wireless Compon. Lett.*, vol. 30, no. 4, pp. 433–436, Apr. 2020.

[7] S. S. Alja'afreh, C. Song, Y. Huang, L. Xing, and Q. Xu, "A dual-port, dual-polarized and wideband slot rectenna for ambient RF energy harvesting," in *Proc. 14th Eur. Conf. Antennas Propag. (EuCAP)*, Mar. 2020, pp. 1–5.

[8] C. Liu, F. Tan, H. Zhang, and Q. He, "A novel single-diode microwave rectifier with a series band-stop structure," *IEEE Trans. Microw. Theory Techn.*, vol. 65, no. 2, pp. 600–606, Feb. 2017.

[9] P. Wu et al., "Compact high-efficiency broadband rectifier with multi-stage-transmission-line matching," *IEEE Trans. Circuits Syst. II, Exp. Briefs*, vol. 66, no. 8, pp. 1316–1320, Aug. 2019.

[10] P. Wu, S. Y. Huang, W. Zhou, and C. Liu, "One octave bandwidth rectifier with a frequency selective diode array," *IEEE Microw. Wireless Compon. Lett.*, vol. 28, no. 11, pp. 1008–1010, Nov. 2018.

[11] H. S. Vu, N. Nguyen, N. Ha-Van, C. Seo, and M. T. Le, "Multi-band ambient RF energy harvesting for autonomous IoT devices," *IEEE Microw. Wireless Compon. Lett.*, vol. 30, no. 12, pp. 1189–1192, Dec. 2020.

[12] M. Fantuzzi, M. Del Prete, D. Masotti, and A. Costanzo, "Quasi-isotropic RF energy harvester for autonomous long distance IoT operations," in *IEEE MTT-S Int. Microw. Symp. Dig.*, Jun. 2017, pp. 1345–1348.

[13] Z. He, J. Lan, and C. Liu, "Compact rectifiers with ultra-wide input power range based on nonlinear impedance characteristics of Schottky diodes," *IEEE Trans. Power Electron.*, vol. 36, no. 7, pp. 7407–7411, Jul. 2021.

[14] D. Surender, M. A. Halimi, T. Khan, F. A. Talukdar, and Y. M. M. Antar, "A 90° twisted quarter-sectored compact and circularly polarized DR-rectenna for RF energy harvesting applications," *IEEE Antennas Wireless Propag. Lett.*, vol. 21, no. 6, pp. 1139–1143, Jun. 2022.

[15] M. A. Halimi, D. Surender, T. Khan, A. A. Kishk, and S. R. Rengarajan, "A multistepped transmission line matching strategy based triple-band rectifier for RFEH/WPT applications," *IEEE Microw. Wireless Compon. Lett.*, vol. 32, no. 8, pp. 1007–1010, Aug. 2022, doi: 10.1109/LMWC.2022.3162633.

[16] C. Liu, H. Lin, Z. He, and Z. Chen, "Compact patch rectennas without impedance matching network for wireless power transmission," *IEEE Trans. Microw. Theory Techn.*, vol. 70, no. 5, pp. 2882–2890, May 2022.

[17] D. Surender et al., "Semi-annular-ring slots loading for broadband circularly polarized DR-rectenna for RF energy harvesting in smart city environment," *AEU, Int. J. Electron. Commun.*, vol. 147, Apr. 2022, Art. no. 154143.

[18] D. Surender, M. A. Halimi, T. Khan, F. A. Talukdar, and Y. M. M. Antar, "Circularly polarized DR-rectenna for 5G and Wi-Fi bands RF energy harvesting in smart city applications," *IETE Tech. Rev.*, vol. 4, pp. 1–15, May 2021, doi: 10.1080/02564602.2021.1923079.

[19] N. Singh, B. K. Kanaujia, M. T. Beg, M. Siddique, T. Khan, and S. Kumar, "A dual polarized multiband rectenna for RF energy harvesting," *AEU, Int. J. Electron. Commun.*, vol. 93, pp. 123–131, Sep. 2018.

[20] L. Li, X. Zhang, C. Song, and Y. Huang, "Progress, challenges, and perspective on metasurfaces for ambient radio frequency energy harvesting," *Appl. Phys. Lett.*, vol. 116, no. 6, Feb. 2020, Art. no. 060501.

[21] P. E. Glaser, "An overview of the solar power satellite option," *IEEE Trans. Microw. Theory Techn.*, vol. 40, no. 6, pp. 1230–1238, Jun. 1992.

[22] Y. Dong et al., "Beam collecting efficiency analysis in microwave power transmission demonstration system for SSPS," in *Proc. 18th Eur. Microw. Conf. (EuMC)*, Sep. 2015, pp. 6–11.

[23] X. Gu, S. Hemour, L. Guo, and K. Wu, "Integrated cooperative ambient power harvester collecting ubiquitous radio frequency and kinetic energy," *IEEE Trans. Microw. Theory Techn.*, vol. 66, no. 9, pp. 4178–4190, Sep. 2018.

[24] L. Guo, X. Gu, P. Chu, S. Hemour, and K. Wu, "Collaboratively harvesting ambient radiofrequency and thermal energy," *IEEE Trans. Ind. Electron.*, vol. 67, no. 5, pp. 3736–3746, May 2020.

[25] C. H. P. Lorenz et al., "Breaking the efficiency barrier for ambient microwave power harvesting with heterojunction backward tunnel diodes," *IEEE Trans. Microw. Theory Techn.*, vol. 63, no. 12, pp. 4544–4555, Dec. 2015.

[26] A. Sharma, V. Singh, T. L. Bougher, and B. A. Cola, "A carbon nanotube optical rectenna," *Nature Nanotechnol.*, vol. 10, pp. 1027–1032, Sep. 2015.

[27] S. Hemour et al., "Towards low-power high-efficiency RF and microwave energy harvesting," *IEEE Trans. Microw. Theory Techn.*, vol. 62, no. 4, pp. 965–976, Apr. 2014.

[28] X. Gu, L. Guo, S. Hemour, and K. Wu, "Optimum temperatures for enhanced power conversion efficiency (PCE) of zero-bias diode-based rectifiers," *IEEE Trans. Microw. Theory Techn.*, vol. 68, no. 9, pp. 4040–4053, Sep. 2020.

[29] X. Gu, S. Hemour, and K. Wu, "Low thermally activated Schottky barrier rectifier: A new class of energy harvester," in *Proc. IEEE Int. Conf. RFID Technol. Appl. (RFID-TA)*, Sep. 2019, pp. 76–79.

[30] Y. Wang and K. Ma, "Loss mechanism of the SISL and the experimental verifications," *IET Microw., Antennas Propag.*, vol. 13, no. 11, pp. 1768–1772, Sep. 2019.

[31] W. Liang, K. Ma, X. Chen, and Y. Wang, "FR4-based low phase noise SISL VCO using tunable weakly coupled resonators," *IEEE Microw. Wireless Compon. Lett.*, vol. 32, no. 1, pp. 72–75, Jan. 2022.

[32] J. Zhang, K. Ma, Y. Wang, and K. Wang, "An FR4-based K-band 1.0-dB noise figure LNA using SISL technology," *IEEE Microw. Wireless Compon. Lett.*, vol. 32, no. 2, pp. 129–132, Feb. 2022.

[33] C. H. P. Lorenz, S. Hemour, and K. Wu, "Physical mechanism and theoretical foundation of ambient RF power harvesting using zero-bias diodes," *IEEE Trans. Microw. Theory Techn.*, vol. 64, no. 7, pp. 2146–2158, Jul. 2016.

[34] F. Zhao, D. Inserra, G. Gao, Y. Huang, J. Li, and G. Wen, "High-efficiency microwave rectifier with coupled transmission line for low-power energy harvesting and wireless power transmission," *IEEE Trans. Microw. Theory Techn.*, vol. 69, no. 1, pp. 916–925, Jan. 2021.